AT721 Section 7:

Approximate methods of solution

The prolific use of simple models to solve the radiative transfer equation can be entirely understood in terms of the desire to obtain relatively accurate solutions that require very little computational effort and relatively free of complexity. The expediency of the simple approximate solutions is desirable for a number of problems that we encounter in the atmospheric sciences that require an immense number of repeated radiative transfer calculations. We provide two examples to illustrate the scope of these problems. The first is the example of calculating broad-band fluxes as required in global weather forecast and research climate models. A single broad-band flux profile is constructed from several monochromatic solutions of the radiative transfer equation. This might require as many as 180 solutions (e.g. Stephens et al., 2001) which then have to be repeated for each grid-point of the model to produce a global distribution of fluxes. A global model with an intrinsic resolution of 2.5 degree latitude/longitude has 10368 grid-points. This equates to a requirement of more than 186000 solutions for the construction of global broad-band fluxes at a single time step. Another example is in the retrieval of atmospheric properties from satellite radiance data. In this application the solution represents the forward model in the retrieval processes and several evaluations of the solutions are typically required for each observed pixel. In the case of single channel of MODIS (ref here), with a pixel resolution of 1 km, a swath width of (approximately) 2000 km, there are more than 44,000 pixels in a single orbit for a single channel of data.

Simple models also serve another purpose that is too often overlooked. They offer a broader view at the intricate way in which the radiance field depends on the properties of the scattering and absorbing medium therefore providing a way of comprehending the results obtained from more complex methods of solution. It is this latter application that will stressed here.

7.1 The asymptotic nature of the Radiance field

On examination of the equation of transfer, in either its integro–differential or its integral form, one is confronted with the complicating presence of the integral term which involves an integration over the direction variable. In fact if it weren't for this term, the equation of transfer would be but a mere differential equation and the theory of multiple scattering would have been worked out and forgotten long ago. Thus the essence of the simplification that is introduced by the class of simple models discussed here is to approximate, in some way, the angular shape of the radiance field so as to introduce some approximation to this integral term. To this end there is a property of the radiance field that is utilized to great benefit by these approximate methods although it is not often explicitly realized. This property is illustrated in Figs. 7.1a and b in which the zenith radiance distribution is shown on descent into the sea (Fig. 7.1a) and deep in a thick cloud (Fig. 7.1b). It is apparent that this radiance structure approaches some sort of asymptotic form with increasing depth into the "medium" – i.e the angular variation assumes a simple, repeatable structure. Eventually some steady distribution is reached and all radiances decrease at the same exponential rate with increasing depth ultimately shrinking down in size but preserving its shape. It is also apparent that this asymptotic distribution can be described as some simple function of zenith angle.

Given this observation we might therefore propose that the radiance field in this asymptotic domain

has the form

$$I(\vec{r},\hat{\xi}) = f(\vec{r})g(\hat{\xi}) \tag{7.1}$$

where the spatial and angular structures of the radiances separate. The factor $f(\vec{r})$, for example, represents the exponential rate of decay of radiances in the medium and the factor $g(\hat{\xi})$ is the conjectured fixed angular distribution that takes a relatively simple form (refer to our discussion in section 2.x).

7.2 Classifying approximate methods and their domain of relevance

Before describing the methods that make use of this property, the domain diagram shown in Fig. 7.2 demonstrates the validity of the following different types of approximations:

- single scattering
- single and double scattering
- diffusion approximation
- asymptotic approximation as $\tau^* \to \infty$

Figure 7.2 The domain of validity of different approximations is shown for the reflection of vertically incident sunlight in isotropic scattering. Left side: single scattering suffices, heavy shading single plus double scattering suffices. Right side, $\tau^* = \infty$ suffices, heavy shading the diffusion approximation suffices. Drawn are the limits corresponding to 1% deviation from exact value. Dashed curves are where the deviation becomes 5%.

Single scatter theory applies when the volume density is considerably smaller than $\sim 0.1\%$ (volume occupied by particles to volume of medium). When this volume density is 1% or greater then the diffusion approximation not only offers simple and reasonably accurate results but provides some insight into the decay of the light field in the medium. For the range of optical depths in between these limits, full solutions to the RTE are required.

Figure 7.1 (a) The flux distribution on a clear sunny day at two indicated depths in Lake Pend Orielle, Idaho (adapted from Preisendorfer, 1976).These fluxes are defined for a collecting surface inclined at an angle θ as shown in the inset. (b) Measured intensity as a function of zenith angle obtained from a scanning radiometer on an aircraft as it flew through the center of a deep stratiform cloud. The lower curve is the difference between measurement and a simple cosine of zenith angle variation (King et al., 1990).

Two simple methods will now be discussed that make use of the asymptotic property of radiance. The second method to be described is perhaps the more widely used and is known as the two stream approximation. The real benefit of the method lies more in the insight the method offers rather than the simplification of the transfer equation it provides. The first method is the diffusion approximation and provides solutions that are so similar to the two stream method that discussion of it in the same context seems warranted. As we will see, the diffusion approximation is more explicitly dependent on the asymptotic hypothesis than is the two stream approximation.

7.3 The diffusion approximation

We write the general form of the radiative transfer equation as

$$\hat{\xi} \cdot \bigtriangledown I\left(\vec{r},\xi\right) = -\sigma_{ext}(\vec{r}) I\left(\vec{r},\hat{\xi}\right) + I_{*}\left(\vec{r},\hat{\xi}\right) + I_{\epsilon}\left(\vec{r},\hat{\xi}\right) \tag{7.2}$$

where the integral term is written in short–hand form

$$I_{*}(r,\hat{\xi}) = \frac{\varpi_{o}}{4\pi} \int P(r,\hat{\xi},\hat{\xi}') I(r,\hat{\xi}') d\Omega(\hat{\xi}').$$

For reasons that will become apparent shortly, the diffusion approximation characteristically focuses on the description of the quantity

$$U(r) = \frac{1}{4\pi} \int_{\Xi} I(\vec{r},\hat{\xi}') d\Omega(\hat{\xi}').$$

rather than on the intensity $I(\vec{r},\hat{\xi})$ – that is on the density of the total flow at $\vec{r}$ rather than the density confined to some direction $\vec{\xi}$. The quantity $4\pi U(r)$ is referred to as the *actinic flux* and the quantity $U(r)$ is the mean intensity. In (7.2)

$$\sigma_{ext}\left(\vec{r}\right) = \kappa\left(\vec{r}\right) + \sigma_{sca}\left(\vec{r}\right)$$

If we integrate (7.2) over all directions using to the integral operator $\int_{\Xi} \cdots d\Omega\left(\xi'\right)$ then (7.2) reduces to

$$\bigtriangledown \cdot F_{net}\left(r\right) = -a\left(r\right) U\left(r\right) + U_{\epsilon}\left(r\right) \tag{7.3}$$

where we write $U_{\epsilon}\left(\vec{r}\right)$ for $\int_{\Xi}\ I_{\epsilon}\left(\vec{r},\hat{\xi}\right) d\Omega\left(\hat{\xi}\right)$ and we make use of the identify $\int_{\Xi}\ I_{*}\left(\vec{r},\hat{\xi}\right) d\Omega\left(\hat{\xi}\right) = 0$.

To see how we arrive at (7.3), let us consider the plane parallel (azimuthally averaged) counterpart to (7.2), namely

$$\mu\frac{dI}{dz} = -\sigma_{ext}I + \frac{\sigma_{sca}(z)}{2}\int_{-1}^{1} P(\mu,\mu')\,I(\mu')\,d\mu' + I_\epsilon(\mu)$$

and integrate

$$2\pi\int_{-1}^{1}\mu\frac{dI}{dz}d\mu = -\sigma_{ext}2\pi\int_{-1}^{1}Id\mu + \frac{\sigma_{sca}(z)}{2}\,2\pi\int_{-1}^{1}\int_{-1}^{1}P(\mu,\mu')\,I(\mu')\,d\mu'd\mu$$

$$+2\pi\int_{-1}^{1}I_\epsilon(\mu)d\mu$$

which in recognizing the definition of F_{net} reduces to

$$\frac{dF_{net}}{dz} = -\sigma_{ext}(z)U(z) + \sigma_{sca}(z)U(z) + U_\epsilon(z)$$

by virtue of the phase function normalization condition. Since $\sigma_{ext} = a(z) + s(z)$ we thus obtain

$$\frac{dF_{net}}{dz} = -\kappa(z)U(z) + U_\epsilon(z)$$

Equation (7.3) contains two unknown quantities, namely F_{net} and $U(z)$ and thus cannot be solved without further information about how each is related to the other. In the diffusion approximation, we make the assumption that $F_{net}(\vec{r})$ shall be proportional to $-\bigtriangledown U$, and that the proportionality constant is the diffusion coefficient d (which will be taken as constant). That is we invoke *Fick's law*

$$F_{net}(r) = -d\bigtriangledown U(\vec{r}) \tag{7.4}$$

As we discuss below, the closer $\varpi_o \to 1$, the better (7.4) becomes. Also, (7.4) increases in accuracy with distance from the boundaries of the medium (Fig. 7.3).

Substitution of (7.4) into (7.3) yields the desired scalar diffusion equation for $U(r)$ of the form

$$-\bigtriangledown\cdot[d\bigtriangledown U(\vec{r})] = -\kappa(\vec{r})U(\vec{r}) + U_\epsilon(\vec{r}) \tag{7.5}$$

or

$$-d\bigtriangledown^2 U(\vec{r}) = -\kappa(\vec{r})\,U(\vec{r}) + U_\epsilon(\vec{r}) \tag{7.6}$$

which can now be solved for $U(\vec{r})$. In order to extract the desired hemispheric flux information we need to introduce further assumption about the intensity field

7.1.1 Radiance distribution in diffusion theory

Figure 7.3 Illustration of the relevance of Fick's law – calculations of F_{net} and U in a two dimensional cloud. The arrows denote the sense of the direction of the net flux and the contours are of U (Gabriel, 1993 personnel comm). Fick's law applies in those regions where the arrows point perpendicularly to the U contours.

According to the observation that the shape of the radiance field is invariant deep in a thick cloud and has a simple structure, let us propose that the radiance field is separable in the sense that

$$I(\vec{r}, \hat{\xi}) = f\left(\vec{r}\right) g\left(\hat{\xi}\right)$$

and more specifically that a spherical harmonics expansion is an appropriate representation of the field. Thus we approximate

$$I\left(\vec{r}, \hat{\xi}\right) = \sum_{n=0}^{\infty} \sum_{m=n}^{n} F_n^m\left(\vec{r}\right) \phi_n^m\left(\hat{\xi}\right) \tag{7.7}$$

where

$$\Phi_n^m\left(\hat{\xi}\right) = \left[\frac{2n+1}{4\pi} \frac{(n-m)\,!}{(n+m)\,!}\right]^{1/2} P_n^m\left(\mu\right) e^{im\phi}$$

$$F_n^m\left(\vec{r}\right) = \int_0^{2\pi} \int_{-1}^{1} I(\vec{r}, \mu, \phi)\ \Phi_n^m(\mu, \phi) d\mu d\phi$$

For example and in keeping with our interest in fluxes, we use only the first two terms in the expansion for $m = 0$

$$I = F_0^0 \phi_0^0 + F_1^0 \phi_1^0$$

where

$$F_0^0(z) = \left(\frac{1}{4\pi}\right)^{1/2} U(r), \qquad \phi_0^0 = \left(\frac{1}{4\pi}\right)^{1/2} P_0^0(\mu)$$

$$F_{net}(z) = \left(\frac{4\pi}{3}\right)^{1/2} F_1^0(z) \qquad \phi_1^0 = \left(\frac{3}{4\pi}\right)^{1/2} P_1^0(\mu)$$

so it follows that

$$I\left(z,\mu\right) = \left(\frac{1}{4\pi}\right)^{1/2} F_0^0(z) + \left(\frac{3}{4\pi}\right)^{1/2} \mu F_1^0(z)$$

or in terms of U and F_{net}

$$I\left(z,\mu\right) = \frac{1}{4\pi}\left[U\left(z\right) + 3\mu F_{net}\left(z\right)\right] \tag{7.8}$$

This form of intensity function provides a relatively mild structure dependence on μ (Fig. 7.2) but it is one that nevertheless is observed in real clouds. Using (7.4) we cast (7.8) into a form involving only $U(z)$

$$I\left(z,\mu\right) = \frac{1}{4\pi}\ \left[U\left(z\right) - 3d\mu \bigtriangledown U\left(z\right)\right] \tag{7.9}$$

Now we can estimate d using the following steps:

- substitute (7.9) into (7.1)
- introduce the two term expansion of the of the phase function as

  $$p(\mu,\mu') = 1 + 3g\mu\mu'$$

  and carry out the integrals of the path radiance term, then the value of d is

  $$d = \left[3\sigma_{ext}(1 - g\varpi_o)\right]^{-1} \tag{7.10}$$

  and with $g \sim 0.8 - 0.85$ and $\tilde{\omega}_o \sim 1$ for terrestrial clouds, then $d \approx 2/\sigma_{ext}$

7.1.2 Boundary conditions

Figure 7.4 Geometry illustrating the problems of boundary conditions in the diffusion domain.

The boundary condition that we usually invoke is the diffuse intensity $I(\vec{r},\hat{\xi})=0$ for intensity entering the medium. Here we encounter a problem with the diffusion approach. Consider Fig. 7.4 and define the inward normal as $\hat{n}$ at point $\vec{r}$. Thus the condition required is:

$$I(\vec{r},\hat{\xi})=0 \quad \hat{\xi}\cdot\hat{n}<0 \tag{7.11}$$

According to (5.8) however, the intensity has a simple angular distribution, namely

$$I(\vec{r},\hat{\xi})=\underbrace{\frac{1}{4\pi}U(\vec{r})}_{>0}+\underbrace{\frac{3}{4\pi}\hat{\xi}\cdot\hat{n}F_{net}(\vec{r})}_{\leq 0,\geq 0}$$

The first term is always positive definite whereas the second term assumes either sign depending on the sign of F_{net} (usually >0 at the boundary point $\vec{r}$). Thus our condition cannot be satisfied exactly and some type of approximate boundary condition must be considered. Consider the geometry of a stratified atmosphere to fix ideas

$$F^{-}(z)=0 \text{ at } z=a \text{ and for } \hat{\xi}\cdot\hat{n}=-\mu<0$$

Since

$$F_{net}(z)=\int_0^{2\pi}\int_{-1}^{1} I(r,\mu',\phi')\mu' d\mu' d\phi' = F^{+}(z)+F^{-}(z)$$

it follows that

$$F_{net}=F^{+}$$

such that the approximate boundary condition at $z=a$ is

$$I(z=a,-\mu)=\frac{U}{4\pi}-\frac{3\mu F^{+}}{4\pi}=0 \tag{7.12}$$

and on substitution of (7.4) into (7.12) yields

$$I(z=a,-\mu)=U+\frac{2\mu}{3\sigma_{ext}\left(1-\varpi_o g\right)}\,\frac{dU}{dz}=0 \tag{7.13}$$

One way of assessing the error associated with the approximate boundary condition is to compare (5.13) to a particular problem for which we know the exact solution - the Milne problem. For this case (semi-infinite atmosphere, isotropic scattering), the diffusion satisfies the boundary condition

$$U+\frac{0.7104}{\tilde{\omega}_o\sigma_{ext}}\,\mu\,\frac{dU}{dz}=0 \tag{7.14}$$

within 0.7% for $0.6\leq\tilde{\omega}_o\leq 1$. Thus it is clear that (7.13) is only an approximation to (7.14) where the factor $2/3\sigma_{ext}\left(1-\varpi_o g\right)$ approximates $0.7104/\varpi_o\sigma_{ext}$. Clearly for the isotropic case ($g=0$), the factor $2/3\sigma_{ext}$ approximates the Milne factor best for $\varpi_o\to 1$ (i.e., the particles that are mostly scattering rather than absorbing).

7.1.3 Simple solutions using diffusion theory

Let us consider a plane parallel, sourceless atmosphere with $U_\epsilon=0$ and suppose we are deep in the medium. Thus the diffusion equation of relevance follows from (7.6) as

$$d\bigtriangledown^2 U-\kappa U=0$$

which admits solutions of the form

$$U(z) = C_+ e^{\lambda z} + C_- e^{-\lambda z} \tag{7.15}$$

where

$$\lambda = \sqrt{\frac{\kappa}{d}} = \sqrt{3\kappa\left(\sigma_{ext} - g\sigma_{sca}\right)}$$

and C_+ and C_- are boundary conditions. It can be simply demonstrated that

$$\lambda < \sigma_{ext}$$

which suggests that transmission of diffuse radiation exceeds that associated with direct beam attenuation.

(a) Infinitely thick medium

Deep in an infinitely thick medium, the approximate form of (7.l5) is

$$U(z) = C_- e^{-\lambda z} = U(0) e^{-\lambda z} \tag{7.16}$$

since $C_+ = 0$. Thus it follows that

$$\frac{dU}{dz} = -\lambda U\left(z\right)$$

and when substituted into (7.9)

$$I(z,\mu) = \frac{U\left(z\right)}{4\pi}\left[1 - 3\lambda d\mu\right] = \frac{U\left(0\right)}{4\pi}\ D_p\left(\mu\right) e^{-\lambda z} \tag{7.17}$$

where

$$D_p(\mu) = \left[1 - 3\lambda d\mu\right]$$

is the diffusion pattern. For conservative scattering, $\varpi_o = 1, \kappa = 0$ and the diffusion pattern is characterized by isotropic radiance field. Fig. 7.5 shows examples of the diffusion pattern for different values of ϖ_o as a function of μ.

Figure 7.5 The diffusion pattern as a function of μ for a H–G phase function with $g = 0.85$ and for seven values of single scattering albedo.

(b) Finitely thick layer $\Delta z = z^*$
Using (7.15), it follows that at

$$\begin{aligned} z = 0 \quad &: \; U(0) = C_+ + C_- \\ z = z* \quad &: \; U(z^*) = C_+ e^{\lambda z^*} + C e^{-\lambda z^*} \\ &\quad C_\pm = \pm \frac{U(z^*) - U(0) e^{\mp \lambda z^*}}{e^{\lambda z^*}} - e^{-\lambda z^*} \end{aligned} \tag{7.18}$$

where again from (7.9)

$$I(z, \mu) = \frac{C_+}{4\pi} D_p(\mu) e^{\lambda z} + \frac{C_-}{4\pi} D_p(-\mu) e^{-\lambda z}$$

where

$$D_p(\pm\mu) = 1 \pm 3\lambda d\mu$$

[*Reference King, 1981: A method for determining the single scattering albedo of Clouds Through Observations of the Internal Scattered Radiation Field, J. Atmos. Sci.*, **38**, 2031-2044.] The angular distribution of the intensity deep in a thick cloud is defined by the diffusion pattern. As we have already noted, this pattern varies as a simple function of μ. The amplitude of this variation is directly proportional to $d\lambda$ (Fig. 7.5), which by definition is

$$\lambda = [3(1 - \varpi_o)(1 - \varpi_o g)]^{1/2} \sigma_{ext}$$

where we define the factor

$$\sqrt{3} d\lambda = s = \left(\frac{1 - \varpi_o}{1 - \varpi_o g} \right)^{1/2}$$

is know as the *similarity parameter*. Two important aspects relating to s require comment:

- the angular structure of the radiance field within the diffusion domain in two clouds is the same when s is the same. By scaling the extinction we can convert a problem of anisotropic scatter to one of isotropic scatter.
- Measurements of D_p, and an estimate of g provides a means of determining ϖ_o (Fig. 7.6)

Figure 7.6 The spectrum of s and ϖ_o derived from calculations and the estimates of these parameters using measurements of the intensity in clouds from an instrument that scans from zenith to nadir.

7.4 The two stream approximation

While it is possible to approach the development of the two stream equations in a number of different ways, the end result is always the same, namely that we arrive at equations of the form

$$\frac{d}{d\tau}\begin{pmatrix} F^+ \\ F^- \end{pmatrix} = \begin{pmatrix} t & -r \\ r & -t \end{pmatrix} \begin{pmatrix} F^+ \\ F^- \end{pmatrix} + \begin{pmatrix} \Sigma^+ \\ \Sigma^- \end{pmatrix} \tag{7.19}$$

or as

$$\frac{d}{d\tau}F = AF + \Sigma \tag{7.20}$$

which is merely another expression of (4.20). For the problems of solar radiative transfer

$$\Sigma^{\pm}_{sol}(\tau) = \pi F_{\odot}\varpi_o X^{\pm}_{\odot} e^{-\tau/\mu_{\odot}} \tag{7.21}$$

and for problems of infrared transfer

$$\Sigma^{\pm}_{IR}(\tau) = b_0 + b_1\tau \tag{7.22}$$

The two stream coefficients r, t, and $X^{\pm}_{\odot}$ define particular forms of the two stream approximation (or 'model'). Common forms of these coefficients and the two stream model they define are given in Table 7.1. The detailed derivation of the coefficients of the Eddington approximation are provided in the appendix

Table 5.1 Different two stream approximations and the corresponding coefficients

Model	**t**	**r**	$X_{\odot}^{+}$
Eddington	$\frac{1}{4}[7-\varpi_o(4+3g)]$	-$\frac{1}{4}[1-\varpi_o(4-3g)]$	$-\frac{1}{4}[2-3g\mu_{\odot}]$
Quadrature	$\sqrt{3}[2-\varpi_o(1+g)]/2$	$\sqrt{3}\varpi_o(1-g)]/2$	$-\frac{1}{2}[1-\sqrt{3}g\mu_{\odot}]$
Hemi. constant	$2[1-\varpi_o\beta]$	$2\varpi_o\beta$	$\beta_{\odot}$

where $X_{\odot}^{-}=1-X_{\odot}^{+}$, and for $p(\mu,\mu')=1+3g\mu\mu'$,$\beta=1+3g\mu/2$, $\beta_{\odot}=1+3g\mu_{\odot}/2$.

7.4.1 Fundamental solution

Figure 7.7 The geometric setting for the general solution of the two stream equations.

The general solution follows formally the steps described in chapter 3 in construction of the integral equation. The solution begins with the pre-multiplication of (7.20) by the integrating factor $\exp[-\mathbf{A}t]$ leading to

$$\exp[-\mathbf{A}t]\frac{d\mathbf{F}}{dt}=\exp[-\mathbf{A}t]\mathbf{A}\mathbf{F}+\exp[-\mathbf{A}t]\Sigma(t)$$

and with re-arrangement

$$\frac{d\exp[-\mathbf{A}t]\mathbf{F}}{dt}=\exp[-\mathbf{A}t]\Sigma(t)$$

Integration of this equation yield

$$\mathbf{F}(\tau)=\underbrace{\exp[\mathbf{A}\tau]\mathbf{F}(0)}+\underbrace{\int_0^{\tau}\exp[-\mathbf{A}(t-\tau)]\Sigma(t)dt} \tag{7.23}$$

homogenoussoution particularsolution

where we note that the homogeneous component of the solution represents that part of the radiative transfer that occurs without any contributions by the sources whereas the particular solution represents that contribution to the transfer directly due to sources.

Properties of the 2 stream **A** matrix

$$\mathbf{A} = \begin{pmatrix} t & -r \\ r & -t \end{pmatrix}$$

$$\mathbf{A}^2 = \begin{pmatrix} t^2 - r^2 & 0 \\ 0 & t^2 - r^2 \end{pmatrix} = \lambda^2 \begin{pmatrix} 1 & 0 \\ 0 & 1 \end{pmatrix}$$

$$\mathbf{A}^2 = \lambda^2 \mathbf{A}$$

where $\lambda^2 = t^2 - r^2$. It follows that the expansion (4.x)

$$e^{\mathbf{A}x} = \mathbf{E} + \mathbf{A}x + \frac{\mathbf{A}^2}{2}x^2 + \frac{\mathbf{A}^3}{3}x^3 + \ldots$$

$$= \mathbf{E} + \mathbf{A}x + \frac{\lambda^2 x^2}{2}\mathbf{E} + \frac{\lambda^2 x^3}{3}\mathbf{A} + \ldots$$

$$= (1 + \frac{\lambda^2 x^2}{2} + \frac{\lambda^4 x^4}{4} + \ldots)\mathbf{E}$$

$$+(x + \frac{\lambda^2 x^3}{3} + \frac{\lambda^3 x^5}{5} + ldots)\mathbf{A}$$

$$= \cosh \lambda x \mathbf{E} + \frac{\sinh \lambda x}{lambda}\mathbf{A}$$

where

$$\cosh \lambda x = \frac{1}{2}(e^{\lambda x} + e^{-\lambda x}), \sinh \lambda x = \frac{1}{2}(e^{\lambda x} - e^{-\lambda x}),$$

and therefore

$$e^{\mathbf{A}x} = \frac{1}{2}(e^{\lambda x} + e^{-\lambda x}) \begin{pmatrix} 1 & 0 \\ 0 & 1 \end{pmatrix} + \frac{1}{2\lambda}(e^{\lambda x} - e^{-\lambda x}) \begin{pmatrix} t & -r \\ r & -t \end{pmatrix}$$

$$= \begin{pmatrix} \frac{1}{2}(1 + \frac{t}{\lambda})e^{\lambda x} + \frac{1}{2}(1 - \frac{t}{\lambda})e^{-\lambda x} & -\frac{r}{2\lambda}(e^{\lambda x} - e^{-\lambda x}) \\ \frac{r}{2\lambda}(e^{\lambda x} - e^{-\lambda x}) & \frac{1}{2}(1 - \frac{t}{\lambda})e^{\lambda x} + \frac{1}{2}(1 + \frac{t}{\lambda})e^{-\lambda x} \end{pmatrix} \quad (7.24)$$

7.4.2 The homogeneous solution, the Interaction Principle and Global reflection and transmission functions

The homogeneous portion of the general solution (7.23) can be constructed from the interaction principle written for a sourceless slab medium extending from $0 \rightarrow \tau$. In flux form, the interaction principle (5.x) becomes

$$F^+(0) = TF^+(\tau) + RF^-(0)$$

$$F^-(\tau) = RF^+(\tau) + TF^-(0)$$

which can be re-arranged as follows

$$\begin{pmatrix} F^+(\tau) \\ F^-(\tau) \end{pmatrix} = \begin{pmatrix} T^{-1} & -T^{-1}R \\ RT^{-1}T - RT^{-1}R & \end{pmatrix} \begin{pmatrix} F^+(0) \\ F^-(0) \end{pmatrix}$$

where we can readily identify this expression as the homogeneous part of the solution in (7.23) and further that

$$e^{\mathbf{A}\tau} = \begin{pmatrix} T^{-1} & -T^{-1}R \\ RT^{-1}T - RT^{-1}R & \end{pmatrix} \tag{7.25}$$

Thus by matching each element of (7.25) with the respective elements of (7.24) produces:

$$R(0,\tau) = \tag{7.26a}$$

$$T(0,\tau) = \frac{2e^{-\lambda\tau}}{(1+\frac{t}{\lambda}e^{\lambda\tau} + \frac{1}{2}(1-\frac{t}{\lambda})e^{-\lambda\tau}} \tag{7.26b}$$

for the reflection and transmission of a slab of optical depth τ. These functions have the following properties
•They are bounded between 0 and 1
•They are intrinsically stable as $\tau \to \infty$ such that

$$R(0,\tau) = R_\infty \to \frac{r}{\lambda + t}$$

$$T(0,\tau) = T_\infty \to 0$$

where R_∞ and T_∞ are the reflection and transmission properties of a semi-infinite layer. The semi-infinite reflection is determined solely by the intrinsic scattering and absorption properties of the layer that establish the define r, t and λ.

7.4.3 Particular solutions and the interaction principle

By substituting a specific analytic form for $\Sigma(t)$, such as either (7.21) or (7.22), into the particular solution

$$\int_0^\tau \exp[-\mathbf{A}(t-\tau)]\Sigma(t)dt$$

and with the assumption the matrix $\mathbf{A}$ is constant over the interval $0 < t < \tau$, then we can evaluate this integral analytically. For the solar source terms

$$\int_0^\tau \exp[-\mathbf{A}(t-\tau)]\Sigma(t)dt = \pi F_\odot \varpi_o \int_0^\tau \exp[-\mathbf{A}(t-\tau)]\mathbf{X}_\odot e^{-t/\mu_\odot}dt \tag{7.27}$$

where

$$\mathbf{X}_\odot = \begin{pmatrix} X_\odot^+ \\ X_\odot^- \end{pmatrix}$$

Integration of (7.27) then follows as

$$\pi F_\odot \varpi_o \int_0^\tau \exp[-\mathbf{A}(t-\tau)]\mathbf{X}_\odot e^{-t/mza}dt = \pi F_\odot \varpi_o [\frac{1}{\mu_\odot}\mathbf{E} - \mathbf{A}]^{-1}\mathbf{X}_\odot e^{-t/\mu_\odot}$$

where

$$[\frac{1}{\mu_\odot}\mathbf{E} - \mathbf{A}]^{-1} = \begin{pmatrix} \frac{1/\mu_\odot - t}{\lambda^2 - (1/\mu_\odot)^2} & \frac{r}{\lambda^2 - (1/\mu_\odot)^2} \\ \frac{-r}{\lambda^2 - (1/\mu_\odot)^2} & -\frac{1/\mu_\odot - t}{\lambda^2 - (1/\mu_\odot)^2} \end{pmatrix}$$

and $\mathbf{E}$ is the identity matrix.

For sources of the form (7.22),

$$\int_0^\tau \exp[-\mathbf{A}(t-\tau)]\Sigma(t)dt = \int_0^\tau \exp[-\mathbf{A}(t-\tau)](b_0 + b_1 t)dt$$
$$= \frac{-b_0(t+r) + b_1}{\lambda^2} + \frac{b_1(t+r)}{\lambda^2}\tau$$

Given these forms of particular solution, we can now derive the global source terms as introduced in section 5.x. TBD

7.6 Performance of two stream models

Fluxes derived using two forms of the two-stream model are compared below to fluxes derived from a 16 stream doubling-adding model. These comparisons are placed within the context of the classification method implied in Fig. 7.2 above. Although many different two-stream versions could have been included, only the results of the constant hemispheric model (CHM) of Coakley and Chylek (1975) and the delta-Eddington model (DEM, Joseph et al., 1976) are presented since these models generally out perform all other models. Shown are flux differences between the two stream models as well as 16 stream model and 4 stream models for reference.

The solar flux differences presented in this section are in the form

$$\Delta F(16) - F(2/4)$$

Assuming the 16 stream solutions are closer representations of truth, the difference values may be interpreted as the absolute error in emergent flux (relative to an incident, collimated flux of unit magnitude) in either the two or four stream model.

Flux differences derived in this way are presented in Fig 7.7a and b respectively for reflected and transmitted fluxes for the three assumed values of solar zenith angles stated. The results are presented in the form of the parameter diagram of Fig. 7.2 and reference to Fig 7.2 is thus useful for interpreting these results. The key points derived from these results are that the solar fluxes derived from the DEM are superior to the CHM and not substantially inferior to the 4 stream model at least for the solar zenith angles $\theta_\odot = 0$ and $\theta_\odot = 45$ and especially in that part of the phase space that determines most of the types of radiative transport problems posed by global models (i.e. along the lower optically thin edge of Fig. 7.2).

Longwave flux differences are derived in a similar manner, namely in terms of the upward flux from the top of the layer in question and the downward flux from the base of the same layer. These flux differences were derived from radiative transfer computations for a single isothermal layer illuminated by a unit flux from below. The comparisons are presented for a single layer characterized by the normalized blackbody flux of 0.45 (relative to the unit incident flux) representing a layer in the mid-troposphere. The magnitudes of these flux differences, multiplied by a factor of 100, thus represent percentage errors in longwave fluxes associated with the scheme in question. The results presented in Fig. 7.8c convey a message similar to that of the solar flux comparisons - namely that 4 stream solutions are only marginally better than two stream solutions except under circumstances of optically thin cloud (Fu et al., 1997). Furthermore, the CHM is superior to the DEM over that portion of the phase space pertinent to the majority of global IR transport problems. The errors typically range between for the range of problems relevant to global models.

Figure 7.7 Fig. 7 8 (a) Differences in the reflected solar fluxes between 2,4 and 16 stream models for 3 different solar zenith angles.

Figure 7.8 (b) as in (a) but for downwelling fluxes

Figure 7.8 (c) as in (a) but for downwelling and upwelling IR fluxes

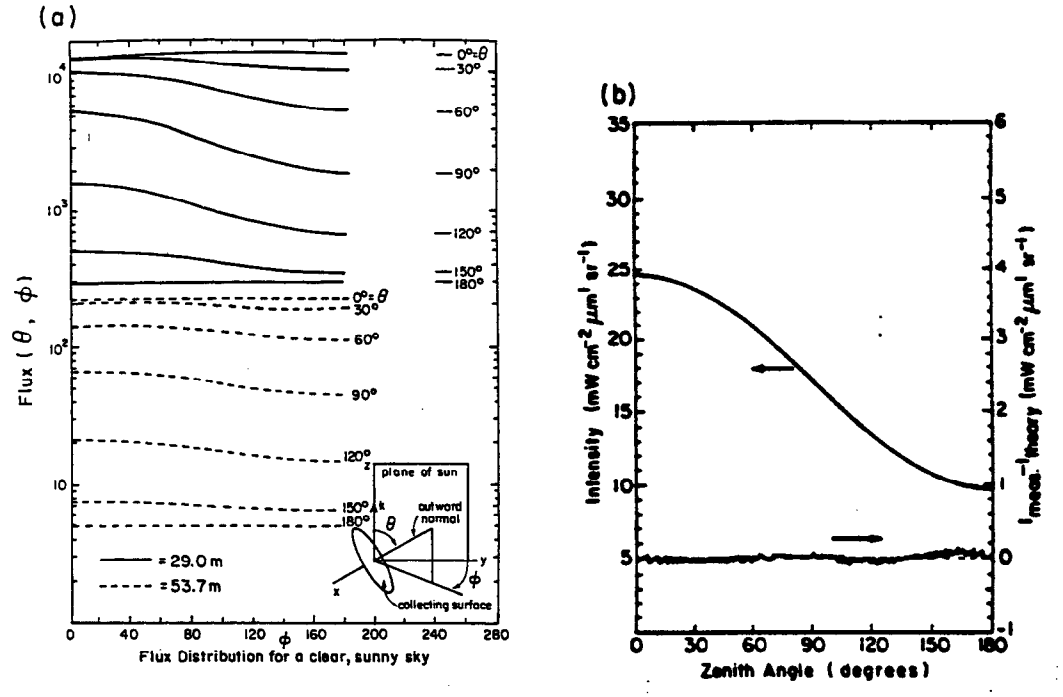

Fig 7.1

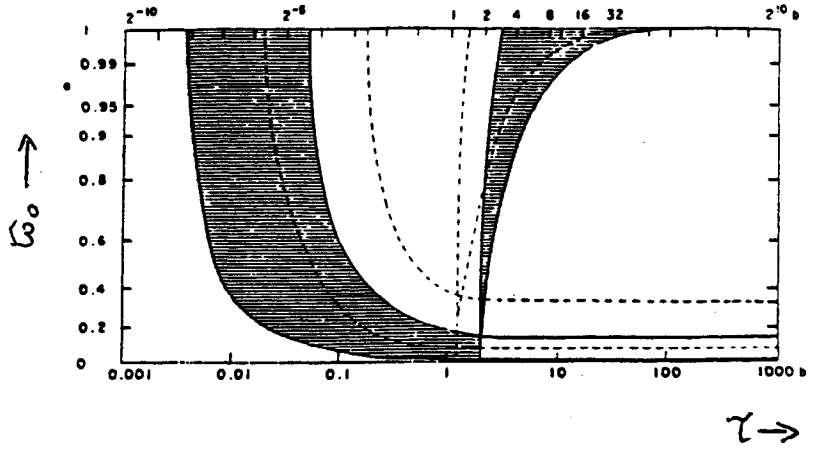

fig 7.2

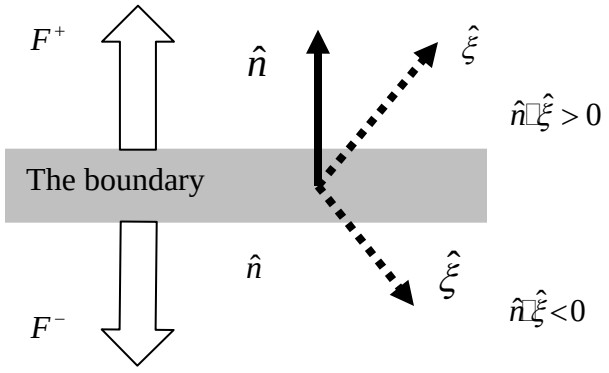

Fig 7.4

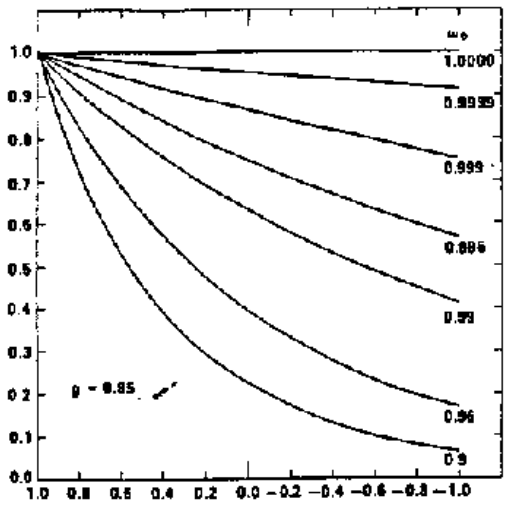
1.0000
0.9999
0.999
0.995
0.99
0.96
0.9
g = 0.85
1.0 0.8 0.6 0.4 0.2 0.0 −0.2 −0.4 −0.6 −0.8 −1.0

fig 7.5

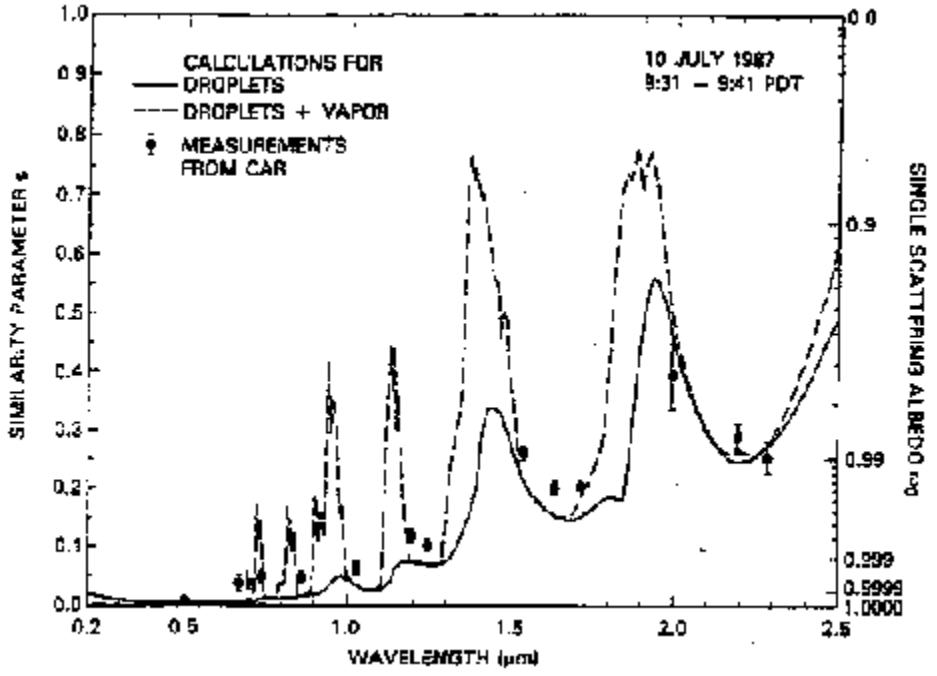
CALCULATIONS FOR
DROPLETS
DROPLETS + VAPOR
MEASUREMENTS FROM CAR
10 JULY 1987
9:31 – 9:41 PDT
SIMILARITY PARAMETER s
SINGLE SCATTERING ALBEDO ω0
WAVELENGTH (μm)
0.2 0.5 1.0 1.5 2.0 2.5
0.99
0.999
0.9999
1.0000

fig 7.6

Table 7.1 Different two stream models and corresponding coefficients

Model	**t**	**r**	$X_{\square}^{+}$
Eddington	$\frac{1}{4}[7-\varpi_0(4+3g)]$	$-\frac{1}{4}[1-\varpi_0(4-3g)]$	$-\frac{1}{4}[2-3g\mu_{\square}]$
Quadrature	$\sqrt{3}[2-\varpi_0(1+g)]/2$	$\sqrt{3}\varpi_0(1-g)/2$	$-\frac{1}{2}[1-\sqrt{3}g\mu_{\square}]$
Hemi. Constant	$2(1-\varpi_0\beta)$	$2\varpi_0\beta$	$\beta_{\square}$

Where $X_{\square}^{-}=1-X_{\square}^{+}$ and for $p(\mu,\mu')=1+3g\mu\mu'$,

$\beta=1+3g\mu/2,\ \ \beta_{\square}=1+3g\mu_{\square}/2,$

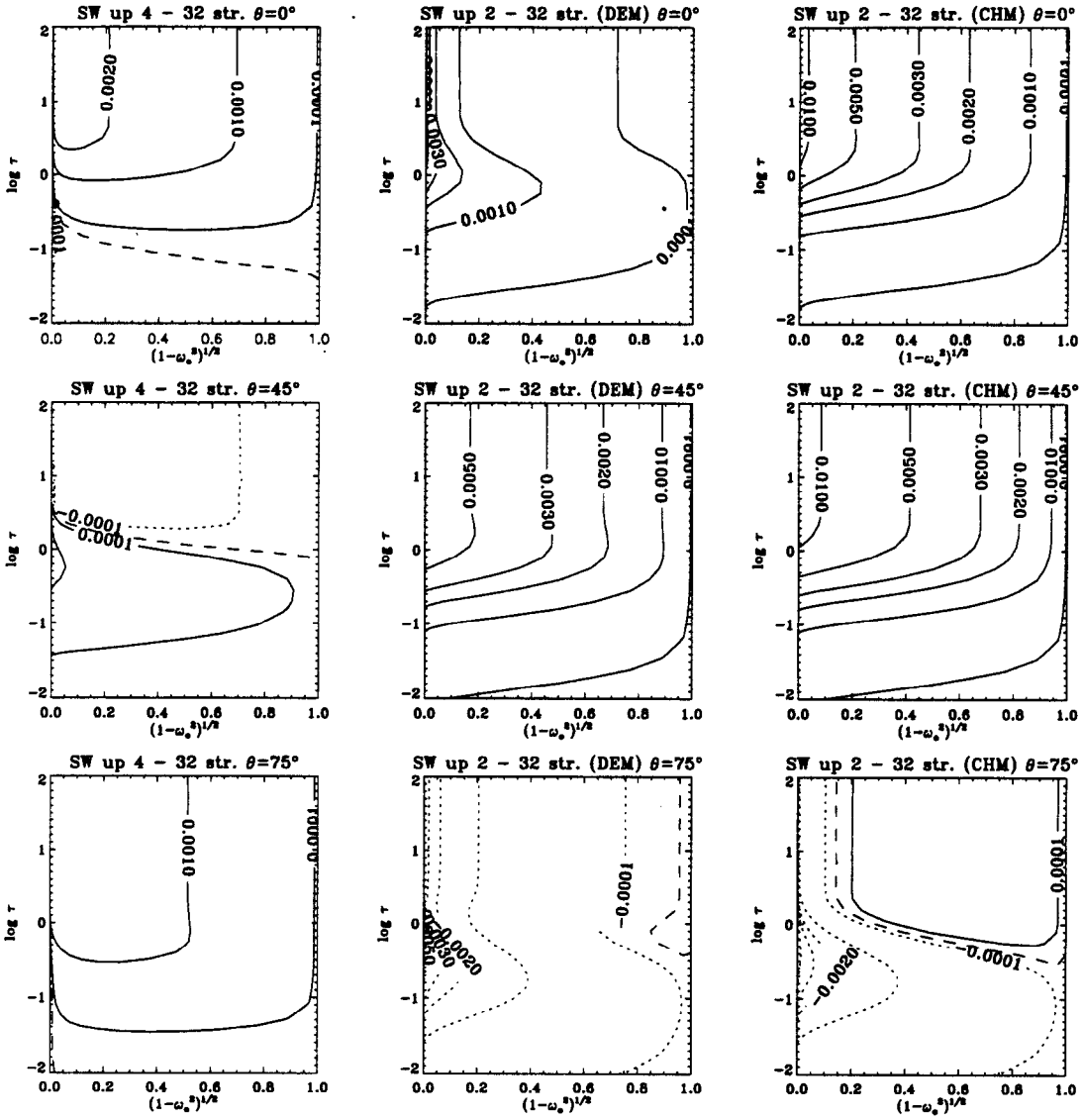
SW up 4 - 32 str. θ=0°
SW up 2 - 32 str. (DEM) θ=0°
SW up 2 - 32 str. (CHM) θ=0°
SW up 4 - 32 str. θ=45°
SW up 2 - 32 str. (DEM) θ=45°
SW up 2 - 32 str. (CHM) θ=45°
SW up 4 - 32 str. θ=75°
SW up 2 - 32 str. (DEM) θ=75°
SW up 2 - 32 str. (CHM) θ=75°
log τ
(1-ω₀ᵍ)^1/2

fig. 7.8

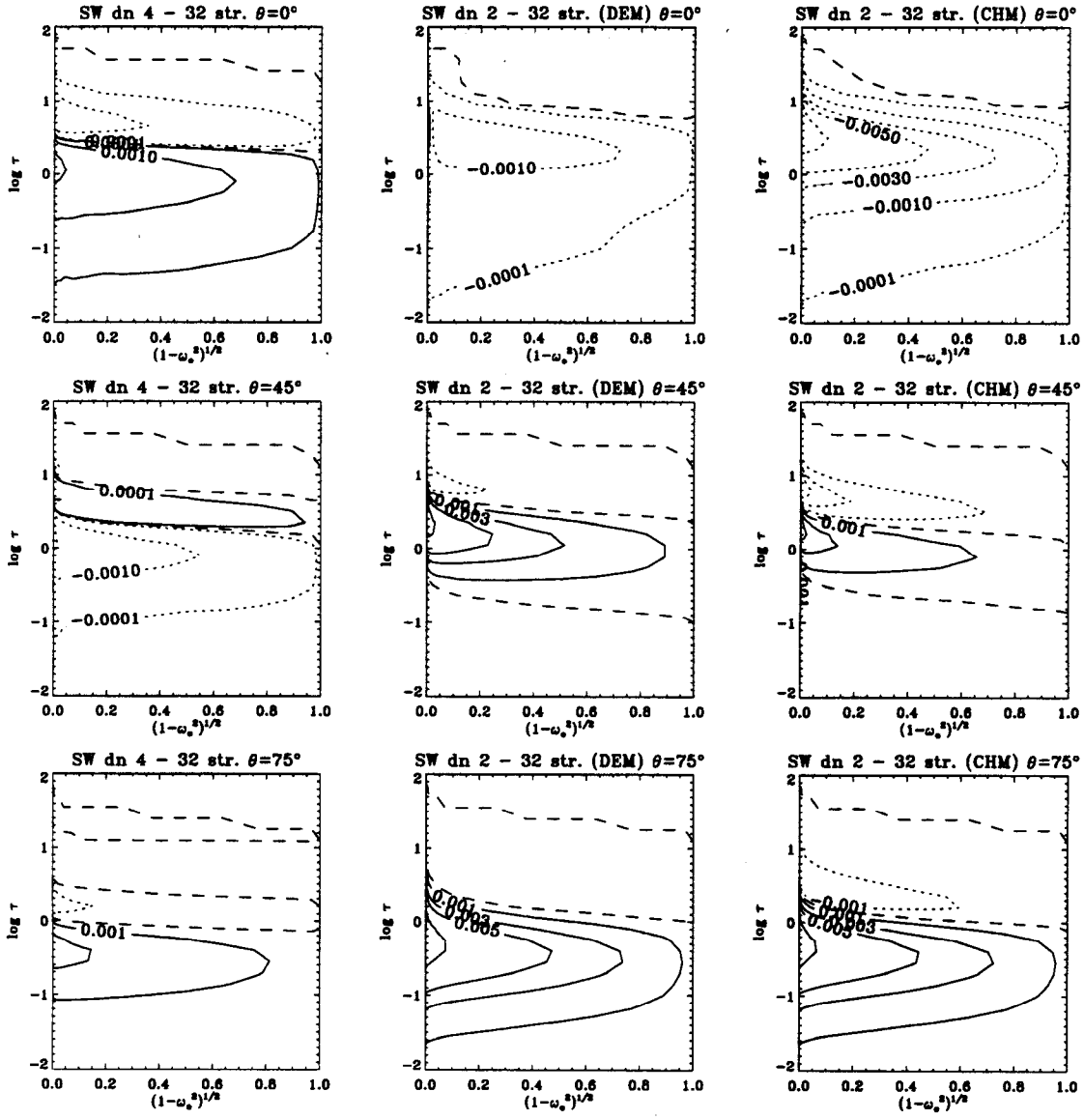
SW dn 4 - 32 str. θ=0°
SW dn 2 - 32 str. (DEM) θ=0°
SW dn 2 - 32 str. (CHM) θ=0°
SW dn 4 - 32 str. θ=45°
SW dn 2 - 32 str. (DEM) θ=45°
SW dn 2 - 32 str. (CHM) θ=45°
SW dn 4 - 32 str. θ=75°
SW dn 2 - 32 str. (DEM) θ=75°
SW dn 2 - 32 str. (CHM) θ=75°
log τ
(1-ω₀²)^1/2

fig.7.7b

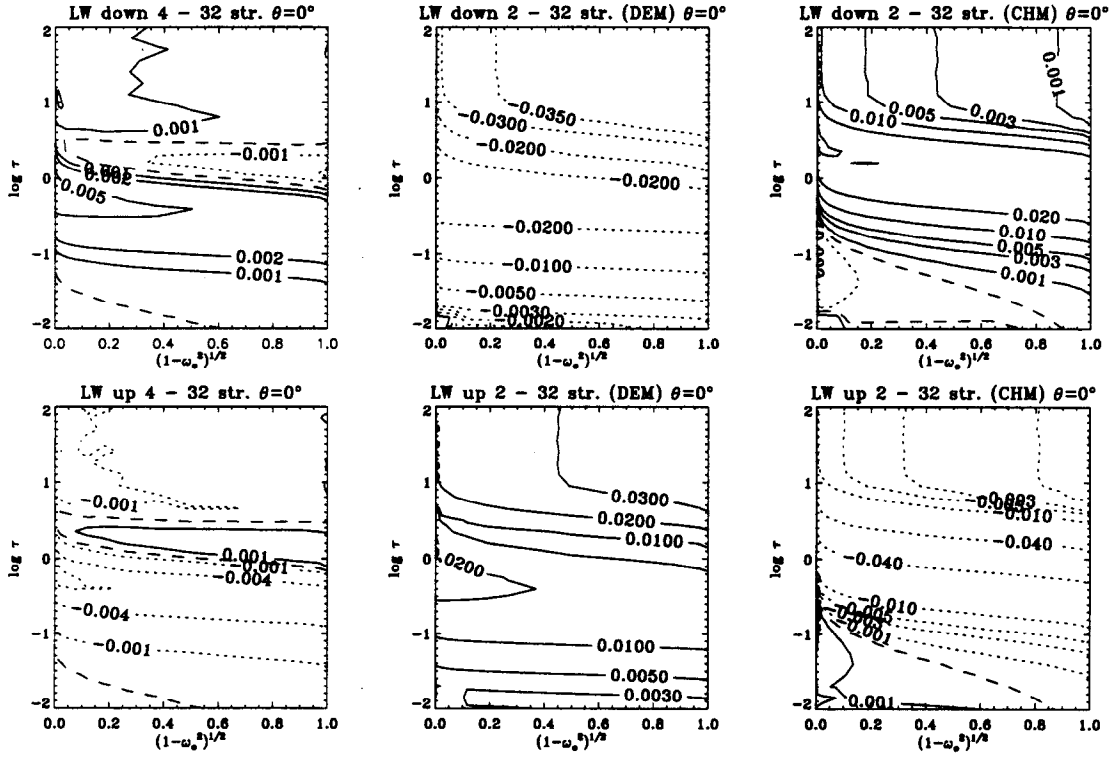
LW down 4 - 32 str. θ=0°
LW down 2 - 32 str. (DEM) θ=0°
LW down 2 - 32 str. (CHM) θ=0°
LW up 4 - 32 str. θ=0°
LW up 2 - 32 str. (DEM) θ=0°
LW up 2 - 32 str. (CHM) θ=0°
log τ
(1-ω₀ˢ)^1/2

fig 7.7c